Multi-energy Microgrids Incorporating EV Integration: Optimal Design and Resilient Operation

Multi-energy Microgrids Incorporating EV Integration: Optimal Design and Resilient Operation

Hasan Masrur, *Student Member, IEEE*, Miadreza Shafie-khah, *Senior Member, IEEE*, M. J. Hossain, *Senior Member, IEEE*, and Tomonobu Senjyu, *Senior Member, IEEE*

***Abstract*—There are numerous opportunities and challenges in integrating multiple energy sources, for example, electrical, heat, and electrified transportation. The operation of multi-energy sources needs to be coordinated and optimized to achieve maximum benefits and reliability. To address the electrical, thermal, and transportation electrification energy demands in a sustainable and environmentally friendly multi-energy microgrid, this paper presents a mixed integer linear optimization model that determines an optimized blend of energy sources (battery, combined heat and power units, thermal energy storage, gas boiler, and photovoltaic generators), size, and associated dispatch. The proposed energy management system seeks to minimize total annual expenses while simultaneously boosting system resilience during extended grid outages, based on an hourly electrical and thermal load profile. This approach has been tested in a hospital equipped with an EV charging station in Okinawa, Japan through several case studies. Following a M1/M2/c queuing model, the proposed grid-tied microgrid successfully integrates EVs into the system and assures continued and economic power supply even during grid failures in different weather conditions.**

***Index Terms*—Multi-energy Microgrids; Resilience; Grid outages; EV; Simulation and optimization.**

I. Introduction

As the traditional natural resource-driven power systems are vulnerable to the climate-induced extreme events such as floods, typhoons and so on, maintaining energy resiliency has become a necessity [1]. The recent rotating grid outages in Texas caused by ice storms and extreme cold remind us that we should not depend solely on the utility, but instead protect and enhance our power and energy system resilience through the use of distributed onsite energy resources (DER). In these instances, microgrids, especially multi-energy microgrids (mMGs), have evolved as vital sources of power supply consistency [2]–[4] .

In order to provide a resilient, effective, and reliable power supply, there is a strong push for the production of optimal energy generation and the use of configurations for modern interconnected systems that consider multiple energy sources. Integrated mMGs have made significant strides in incorporating the use of traditional power sources, renewable energy generators, and energy storage to meet energy needs in all industries. In line with this development, the term 'microgrid resiliency' is coined and has attracted attention in the integrated energy systems literature, with resilience-driven prevention and response strategies leveraging optimization methods, resiliency metrices and scenarios, control techniques, and objectives [5], [6].

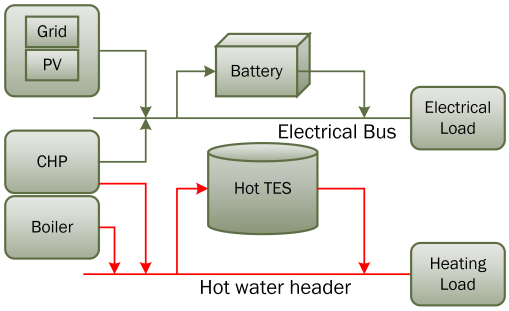

Fig. 1. Schematic diagram of a multi-energy microgrid

The provision of heat and electricity energy is a strongly connected co-optimization task, which is one of the problems for designing and operating the multi-energy system. A schematic of a multi-energy microgrid system is depicted in Fig 1. The combined heat and power (CHP) unit contributes to the high coupling of heating and electrical energy. Several optimization and resilience metrics are presented in the existing literature. Hussain et al. presented an optimization scheme and a resilience index that successfully satisfied the critical load demand during the blackout period by considering uncertainties and incremental costs within three different network topologies [7]. Reference [8] also considered minimization of load curtailment, cost reduction, and local load supply as resilience measures to ensure optimal scheduling of microgrids when the main grid was down. Even so, these articles did not take into account both electrical and heating load demand. In [9], a methodology was discussed for the mMG, which integrated the electricity and gas network under several main grid interruptions. The proposed bi-level optimization technique enhances the system resiliency by securing the electricity and heat demand in the emergency period with a reduction in the operational cost. However, they did not consider the probability of outage survivability. Focusing on the optimal sizing of the batteries, the proposed operation of networked microgrids in article [10] can maximize the annual profit while ensuring reliability and resiliency under typical and extreme grid outage scenarios, although they did

Manuscript accepted for publication. (*Corresponding author: H. Masrur*)

H. Masrur and T. Senjyu are with the Department of Electrical and Electronic Engineering, Faculty of Engineering, University of the Ryukyus, Okinawa 903-0213, Japan (e-mail: k198676@eve.u-ryukyu.ac.jp; b985542@tec.u-ryukyu.ac.jp).

M. Shafie-khah is with School of Technology and Innovations, University of Vaasa, Finland (e-mail: miadreza.shafiekhah@uwasa.fi).

M. J. Hossain is with School of Electrical and Data Engineering, University of Technology Sydney, Australia (e-mail: jahangir.hossain@uts.edu.au).

not discuss the heating demand. In [11], the optimal design and resiliency of microgrids are discussed without considering heating load and EV penetration. Nonetheless, in exploring the possibility of grid failure, the influence of EV integration on multi-energy (thermal plus electricity demand) microgrids should be examined in order to establish a sustainable and resilient energy system.

Japan, like the rest of the world, is committed to reducing greenhouse gas emissions by a significant amount by 2050, and electric vehicles (EVs) will play a significant role in this effort by replacing fossil fuel-powered automobiles [12]. So, EVs need to be charged using renewable energy, and Japan has been promoting housing-based charging where distributed generators are already available in the form of microgrids [13]. EVs can introduce significant technical issues that can result in additional investment to upgrade grid-connected microgrids. Electricity distribution networks were not built with a high penetration of electric vehicles in mind. Charging electric vehicles at home can dramatically raise our typical demand, putting a strain on the power grid's poles and wires. However, if EV charging/discharging is properly regulated, it may result in more efficient networks, reduced rates, and improved treatment for end-use sectors.

Recently, there has been a surge in studies on EVs incorporated into microgrids. Most studies concentrate on developing reliable EV charging and discharging patterns, control strategies for vehicle-to-grid (V2G) and grid-to-vehicle (G2V), energy management techniques, and power quality issues attributed to DER-based microgrids [14]. While the majority of them are focused on independent operation or integration into homes and community microgrids [15]–[21], some are involved in the electricity markets [22]–[24]. Typically, their main goal remains the same: to run a cost-effective and reliable operation. In some cases, both behind-the-meter and ancillary services affect the optimal co-ordination of these EV-assisted microgrids. For the successful operation of EV integrated microgrids, it is critical to consider the intermittent nature of renewable energy resources as well as variable EV parking behaviors. Several articles such as [25]–[27] can be found that discuss these uncertainties in the context of a real-time energy management strategy. However, they have not considered the impact of grid failures explicitly. On the other hand, although numerous studies can be found discussing the heating and electrical energy dispatch of microgrids, where some consider the resiliency of their proposed model, EVs are not taken into account [7]–[10], [28], [29]. In summary, according to the authors' best knowledge, studies of mMGs that consider EVs and adopt a resilient operation scheme simultaneously are limited, whereas unison of electrical power systems, heat power, and transportation energy could exploit the benefits of multi-energy sources. Further studies are required to fully comprehend the optimal design and operation of multi-energy systems that can offer better efficiency, flexibility, and carbon footprint. Although resilience has been extensively studied in the literature, outage survivability issues require further investigation for a clear understanding of resilience, particularly in integrated mMGs.

To fill this gap, this paper presents a robust sizing method and energy management scheme of a mMG to leverage resilience benefits considering EVs, renewable energy generator-PV, conventional power sources- CHP unit, existing gas boiler, thermal energy storage (TES) and battery. The contribution of this work is threefold:

(1) An extensive modeling of all the power supply units of the proposed microgrid is performed. Optimal sizing and dispatch strategy of each source is modeled aiming at minimum cost after careful consideration of a number of pragmatic constraints, including the network constraints.

(2) A detailed EV charging station is modeled that is integrated into the microgrid using the real-world charging station data of Tokyo, Japan. The M1/M2/c queuing model is used, which reflects the real-world situation of any EV charging station, including arrival rate, charging rate, service time, percentage of vehicles on the road, probability of simultaneous charging, and expected EV charging demand.

(3) Finally, the operation of both electrical and heating energy dispatch is tested under a prolonged grid outage in different seasons and loading conditions, and a resiliency index concerning the probability of outage survival of the microgrid incorporated with EV is developed which has not been reported in the existing literature concurrently. The impact of different percentages of critical load demand on outage survivability is discussed as well.

The remainder of the paper is categorized as follows. Section II describes the system model, section III discusses about EV charging station modelling and Section IV delves into the optimal sizing and operation of a microgrid. Section V presents the results of optimization and simulation, as well as a detailed discussion of case studies. The final section contains concluding remarks and suggested future works.

II. System Model

A. CHP Model

Topping cycle CHP units are modeled so that fuel (natural gas) is converted to electricity and recoverable usable heat. The resulting waste heat is captured from this process and used as hot water throughout the facility. This hot water can be stored in the TES, which is also depicted in the next subsection. The following is the interaction involving heat and electric power generation in a CHP plant [31]:

$$Q_{out} = (\frac{\eta_h}{\eta_e}) P_{out} h_c^f \tag{1}$$

where P_{out} and Q_{out} denotes the electric and heat power generation from the CHP unit, respectively. h_c^f is the consumption rate of the fuel, i.e, natural gas. η_e and η_h are the electric and heat recovery efficiency of the CHP plant. Both fuel burn rate and heat recovery rate can be modeled with efficiency of CHP unit as:

$$R_{e,h} = \ a_{e,h} P_{out} + b_{e,h} \tag{2}$$

where R denotes both the fuel rate and available usable heat for electric (e) and heat generation (h) while a and b are the heat recovery efficiency at full and half loading condition at time t, respectively.

TABLE I
COMPARISON OF THE CURRENT STUDY WITH EXISTING LITERATURE

Ref.	Microgrid System				Grid	EV integration				Resilience Evaluation
	Demand type	Storage	CHP Modeling	Optimization technique		Technique	Charging scheduling	Simultaneous charging probability	Real data	
[11]	Electrical	BES	No	MILP	Yes	No				Yes
[9]	Electrical+Heating	-	Yes	MIBLP	No	No				Yes
[30]	Electrical	BES	No	MILP	Yes	No				Yes
[21]	Electrical	BES	No	MOGA	Yes	Simple charging	Yes	No	No	No
[15]	Electrical+ Heating	BES+TES	Yes	MILP	Yes	Smart and uncontrolled charging	Yes	No	Yes	Yes
[26]	Electrical	BES	No	AMPL	Yes	Controlled and uncontrolled charging; battery swapping	Yes	No	No	No
[24]	Electrical	BES	No	CPLEX	No	market price, arrival time of EVs, and the residual energy level of EVs	Yes	No	No	Yes
[18]	Electrical	BES	No	MINLP	No	optimal location and sizing	No	No	No	No
[19]	Electrical+ Heating	None	Yes	-	Yes	Coordinated charging	yes	Yes	Yes	No
[23]	Electrical	None	No	MINLP	Yes	Charging management system	Yes	No	No	No
Current study	Electrical+ Heating	BES+TES	Yes	MILP	Yes	M1/M2/c queuing and Coordinated charging	Yes	Yes	Yes	Yes

B. Thermal storage model

A single-layered hot water TES tank with a thermocline that divides the supply hot water from the returned water is modelled for this study. A hot water TES can store hot water from the boiler plant or the CHP heat exchange unit. This hot water will be used to meet the hot water demands of the facility. During the first hour of the scenario, stored energy is considered to be 50% of the TES capacity. However, the minimum energy storage value is 10% in normal operating condition. The following equation determines the charging and discharging rates, along with efficiency parameters [32]:

$$X_{t,h+1}^{hs} = X_{th}^{hs} + Z_{th}^{hs,c}\eta^{hs,c} - \frac{Z_{th}^{hs,d}}{\eta^{hs,d}} \quad \forall\ t,h \tag{3}$$

Here, the X^{hs} refers to the capacity and $Z_{th}^{hs,d}$ is the charging (c) and discharging (d) rate of the TES with η^{hs} indicating the efficiency for technology t in time step h. The model determines the size of the TES based on the cost-optimal maximum volume of stored energy. We assume the TES can be fully charged with either hot water or chilled water. Between the maximum and minimum stored energy limits, the capacity of stored hot or chilled water is a function of the water volume stored on the tank's supply side of the thermocline.

C. Modelling of Photovoltaic Module

The Photovoltaic modules converts sunlight into DC electricity. The following equation can be used to measure the PV module's output power (4):

$$P_{PV} = Cp_{PV} * D_{PV}(\frac{Ir}{Ir_{STC}})[1 + \alpha_p(T_c) - T_{c,STC}] \tag{4}$$

where, P_{PV} is the PV module's output power, D_{PV} is the solar PV array's derating factor (%), Cp_{PV} is the PV array's rated capacity (kW), Ir is the solar irradiation on the PV panel's surface (kW/m^2), T_c refers to the PV cell temperature in the current time step (°C), α_p is the temperature coefficient of power (%/°C). Ir_{STC} and $T_{c,STC}$ are values calculated under normal test conditions (STCs) (1kW/m^2, 25°C).

The following equation can calculate the PV efficiency at the maximum power (MPP) and under STCs:

$$\eta_{STC} = \frac{Cp_{PV}}{A_{PV}Ir_{STC}} \tag{5}$$

where η_{STC} represents the PV module's efficiency under normal test conditions (%) and A_{PV} specifies the PV module's surface area (m^2).

D. Battery storage model

Batteries aid to provide reliable and backup power supply particularly when renewable energy sources are unavailable. The battery capacity (Cap_{bat}) must be adapted by the following equation in order to keep enough charge when PV power is unavailable.

$$Cap_{bat} = \left[\frac{E_{load}DA}{\eta_{con}\eta_{bat}DOD}\right] \tag{6}$$

where E_{load} is the average energy demand (kWh/day), DA is the days of autonomy, η_{con} is the efficiency of converter, η_{bat} is the efficiency of battery, and DOD is the depth of charge of the battery. The model does not account for battery cycling deterioration; instead, the battery is assumed to be substituted once throughout the analysis period depending on calendar degradation and factor in accumulated replacement costs.

III. MODELING OF TRANSPORTATION ELECTRIFICATION

In our study, a single EV charging facility was introduced using the M1/M2/c queuing model. In this model, M1 represents the Non-homogeneous Poisson arrival rate at the charging facility. The EV arrival rate is dependent on the quantity of EVs on the road. If the number of vehicles on the road increases, the arrival rate also increases, no matter what the pricing or operational constraints are. The service time of EVs, referred to as M2, follows the exponential distribution and service time is affected by charge level, battery capacity, battery state of charge (SoC), and battery charging behavior (BCB).For charging stations, higher charging power typically begins at full charge and lowers off when the battery SoC is approached, which explains the BCB of EV charging. c denotes the number of chargers at the charging site. For our particular study area, it is expected that arrival at the charging facility is proportionate to the number of vehicles on the roadways. Based on this premise, we assume that EV driving and usage habits are consistent with those of traditional automobiles.

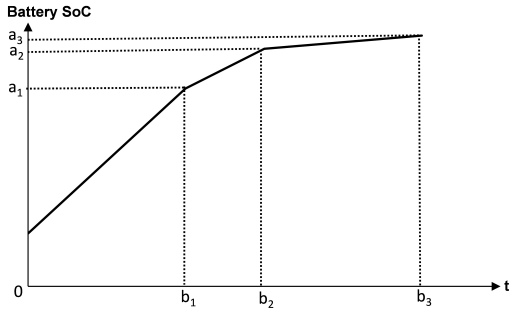

Fig. 2. Piecewise linear approximation for the typical BCB of EV [34].

To charge the battery, the BCB model is employed [33]. First, the charging time of arriving EVs must be estimated using their SoC information. This needed knowing the mileage (V_{M_i}) covered by the EVs. The Tokyo Environmental Public Service Corporation (PEPSC) survey data [13] can be used to estimate this data. EV travel has been proven to follow the long normal distribution, with a mean of 40 miles and a variation of 20 miles [33]. Battery capacity (B_{cap_i}) and energy consumption per mile (E_m) are required in this model. Vehicle type determines the data, and four vehicle classes are included.

The daily energy consumed (E_{c_i}) by each class (i) of EVs can be the calculated as following:

$$E_{c_i} = \begin{cases} B_{cap_i} & \text{, if } V_{M_i} \geq V_{M_i \max} \\ E_{m_i} V_{M_i} & \text{, if } V_{M_i} < V_{M_i \max} \end{cases}, \forall i \tag{7}$$

The maximum driving range of various EV classes is calculated as follows:

$$V_{M\max} = \frac{B_{cap_i}}{E_{m_i}}, \forall i \tag{8}$$

The SoC of the EVs that have arrived at the charging facility can be computed as follows:

$$SoC_i = 1 - \frac{E_{c_i}}{B_{cap_i}}, \forall i \tag{9}$$

To account for the limitation of battery charging characteristics, the SoC of the arriving EVs is considered to be between 0.2 and 0.85. The needed mean charging time can be determined using the piece-wise approximation of battery charging characteristics as shown in Fig. 2 and information about SoC of different classes (y) of EVs. So, the following formula can be used to compute the average charging time:

$$T = \frac{SoC_{iy} - b_y}{a_y}, \forall y \in (1-4), \forall i \tag{10}$$

where, the slope and intercept of each linear element of the battery charging characteristics are a_y and b_y, respectively.

The M1/M2/c queuing analysis is used in order to calculate the probability of a number of simultaneously charging EVs at the charging facility,$P_t(n)$.

$$\begin{gathered} P_t(n) = \frac{\rho^n}{n!} P_t(0), n = 1, 2, \ldots\ldots, c, \forall t \\ P_t(0) = \left[\sum_{n=0}^{c-1} \frac{\rho^n}{n!} + \frac{\rho^c}{c!(1-a)} \right]^{-1}, \forall t \\ \rho = \frac{\lambda}{\mu}, \quad a = \frac{\rho}{c} \end{gathered} \tag{11}$$

where, λ represents for mean inter-arrival time, t (minute), ρ stands for EV occupation rate at charging station, and μ refers to service time in minute. The divide of the occupation rate and the number of EV chargers is indicated by the a symbol.

If the number of EVs arriving at the charging facility exceeds the quantity of chargers, the EVs will have to wait for service. The following equations are used to calculate the likelihood of waiting EVs, $P(n \geq c)$ and the expected waiting time, $\bar{W}$.

$$\begin{gathered} P(n \geq c) = \frac{\frac{\rho^c}{c!}}{(1-a) \sum_{n=0}^{c-1} \frac{\rho^n}{n!} + \frac{\rho^c}{c!}} \\ \bar{W} = \frac{P(n \geq c)}{\mu c (1-a)} \end{gathered} \tag{12}$$

Finally, depending on the frequency of the number of EVs charging at the same time, the total expected charging power can be calculated as follows:

$$\begin{gathered} I_{t,i} = \min \left(\frac{B_{cap_i}}{V_l T_t}, I_{\max} \right) \\ P_{ap_t} = I_{t,i} V_l \\ E\left[P_{ap_t}\right] = \sum_{n=0}^{c} P(n) P_{ap_t}, \forall t \end{gathered} \tag{13}$$

where, V_l refers to the voltage level of the EV charger, I is the charging current and P_{ap_t} is the active power demand from charging EVs.

IV. Modeling of Microgrid: optimal sizing, dispatch strategy and Resilience

This study have used a modified mixed-integer linear program (MILP) to solve the optimization problem. It derives the optimal selection, sizing, and dispatch scheme of power generators for a specific site while assuring the minimum life cycle cost (LCC) over project lifetime. The overall methodology of the proposed multi-energy microgrid is shown in Fig. 3.

A. Objective function

Total equipment expenses for battery, PV, CHP, and thermal storage are included in the objective function.

1) System capital cost: The capital cost associated with generating energy technology (PV, TES and CHP) is given by:

$$C_{et} = \sum_{l \in \mathcal{L}, h \in \mathcal{H}} \left(P_{tlh} c_h^e \right) \tag{14}$$

where, P_{tlh} and c_h^e are the power rating and capital cost for the technology t, serving load l, in time step h.

The battery capital cost of can be determined by [30]:

$$C_{bat} = \sum_{t \in \mathcal{T}} \left(X_t c_t \right) + \left(B^{kWh} c_{kWh}^b \right) + \left(B^{kW} c_{kW}^b \right) \tag{15}$$

where X_t and c_t are the system size and capital cost for energy technology t whereas c_{kWh}^b, c_{kW}^b, B^{kWh}, B^{kW} are referred to the battery size, capacity and associated costs.

The annual system capital cost is the summation of the capital costs of generating technologies and storage:

$$C_{cap} = C_{et} + C_{bat} \tag{16}$$

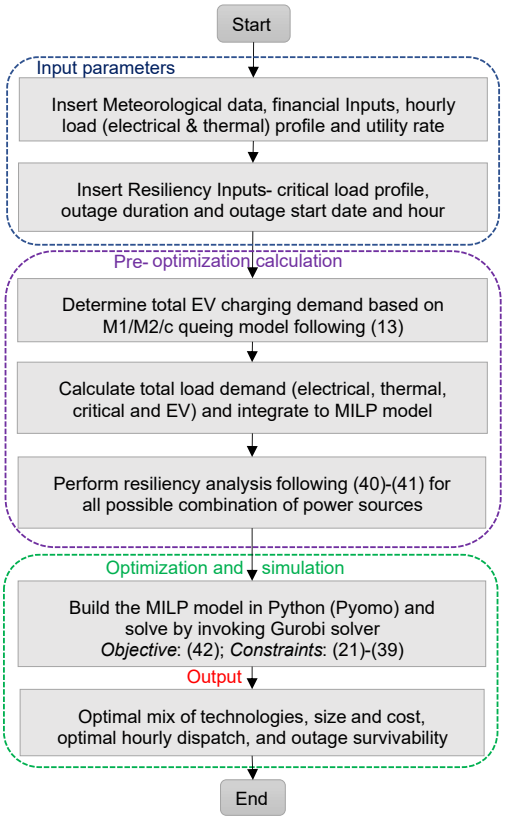

Fig. 3. Overall workflow of the proposed method.

2) Operation & maintenance cost: The O&M cost of the microgrid is expressed as [30]:

$$C_{OM} = \sum_{t \in \mathcal{T}} (X_t c_t^{om}) \tag{17}$$

where c_t^{om} is the O&M cost per unit size of the system for technology t($/kW).

3) Demand cost: The demand cost is defined as [30]:

$$C_{Dn} = \sum_{r \in \mathcal{R}} (d_r c_r^d) + \sum_{m \in \mathcal{M}} (d_m c_m^d) \tag{18}$$

where d_r, d_m are the peak demands while c_r^d and c_m^d represents their demand costs in month m within ratchet r.

4) Grid energy cost: The power purchase cost from grid is calculated by:

$$C_{grid} = \sum_{u \in \mathcal{U}^P, h \in \mathcal{H}^g} X_{uh}^g c_{uh}^g \tag{19}$$

where, X_{uh}^g and c_{uh}^g indicates the imported grid power and its cost in demand tier u during time step h.

5) Total cost: The annual total cost of the system is given by:

$$C_{tot} = C_{cap} + C_{OM} + C_{Dn} + C_{grid} \tag{20}$$

B. System constraints

The life cycle cost is minimized subject to the following constraints:

1) Load constraints:

$$\sum_{t \in \mathcal{T}} (F_{tlh}^{pd} P_{tlh} F_t^{dgr}) \leq L_{lh}, \quad \forall\, h \in \mathcal{H} \tag{21}$$

$$\sum_{l\ \epsilon\ \mathcal{L}} P_{tlh}\ \leq X_{th}, \quad \forall\, h\ \epsilon\ \mathcal{H} \tag{22}$$

where, F_{tlh}^{pd} is the annual production factor, F_t^{dgr} is the degradation factor of the generating source t and L_{lh} indicates the production size limitation. (21) requires the sum of the energy on-site demand to be less than or equal to the maximum load for each phase of all energy sources and (22) states the production constraint that the rated power provided by the PV system has to be equivalent to the system size selected in each phase over all loads [11].

2) Battery charging and discharging: The following equations represent storage restrictions, such as battery charging and discharging, while taking into account degradation and battery state of charge at each time step:

$$B_h^+ = \sum_{t \in \mathcal{T}} (F_{tlh}^{pd} X_t F_t^{dgr} \eta_B), \quad \forall\, h \in\ \mathcal{H} \tag{23}$$

$$B_h^{SOC} = B_{h-1}^{SOC} + B_h^+ - B_h^-, \quad \forall\, h \in \mathcal{H} \tag{24}$$

$$B_h^- \leq B_{h-1}^{SOC}, \quad \forall\, h \in \mathcal{H} \tag{25}$$

$$Z_h^{B^+} + Z_h^{B^-} \leq 1, \quad \forall\, h \in \mathcal{H} \tag{26}$$

where B_h^- = power discharged from the battery in time step h (kW), η_B = battery efficiency, B_h^{SOC}= charge stored in the battery in time step h (kWh), $Z_h^{B^+}$ = 1 if battery is being charged in h time step (else 0), $Z_h^{B^-}$ = 1 if battery is being discharged in h time step (else 0).

3) Demand constraints: The demand rate limitations are described by the next two equations. The demand for each demand period or month must be larger than or equal to the grid electricity used during that period or month [11].

$$\sum_{h \in\ \mathcal{H}_r,\ l\ \in \mathcal{L}} P_{tlh} \leq d_r, \quad \forall\ r \in \mathcal{R} \tag{27}$$

$$\sum_{h\ \epsilon\ \mathcal{H}_m,\ l\ \epsilon\ \mathcal{L}} P_{tlh} \leq d_m, \quad \forall\ m \in \mathcal{M} \tag{28}$$

where, $m \in \mathcal{M}$, $r \in \mathcal{R}$, and $l \in \mathcal{L}$ are the sets of monnths, ratchets, demands and loads, respectively.

4) Fuel constraints: A restriction on the amount of fuel consumed by each fuel type is set by (29) which can be burnt in various ways. (30) employs a linear function to connect the output of a non-CHP, fuel-burning electricity-generating technology to its equivalent usage. According to (31) any non-CHP heating technology's fuel usage is proportionate to its hourly thermal output.

$$\sum_{t \in \mathcal{T}, h \in \mathcal{H}} X_{th}^{\mathrm{f}} \leq g_f^{\mathrm{af}}, \quad \forall f \in \mathcal{F} \tag{29}$$

$$X_{th}^{\mathrm{f}} = h_t^{\mathrm{fm}} P_{th} + h_t^{\mathrm{fb}} Z_{th}^{\mathrm{t_0}}, \quad \forall t \in \mathcal{T}, h \in \mathcal{H} \tag{30}$$

$$X_{th}^{\mathrm{f}} = h_t^{\mathrm{fm}} X_{th}^{\mathrm{hs}}, \quad \forall t \in \mathcal{T}, h \in \mathcal{H} \tag{31}$$

where, X_{th}^{f} indicates the amount of fuel burned, X_{th}^{hs} is the thermal (heat) production, g_f^{af} is the fuel availability, h_t^{fm} is slope of the fuel rate curve, h_t^{fb} is the y-intercept of fuel rate, $Z_{th}^{\mathrm{t_0}}$= 1 if operating in time step h (else 0), for technology t.

5) Thermal constraints: For required thermal CHP systems, (32) states that the rated electricity supplied must equal the rated thermal energy supplied times a predetermined ratio for each time step.

$$\sum_{d\in\mathcal{D},f\in\mathcal{F}} X_{dtlhf}^{rp} = \sum_{d\in\mathcal{D},f\in\mathcal{F}} X_{dtlhf}^{rp} h_t^f \quad \forall t\in\mathcal{T}, l\in\mathcal{L}, h\in\mathcal{H} \tag{32}$$

where, X_{dtlhf}^{rp} indicates the rated power supply and h_t^f refers to the ratio of thermal to electric production for technology t and fuel f.

The limits of charging and discharging power are represented in the following two equations:

$$0 \le P_{th}^{thml,c/d} \le P_{\max,t}^{thml,c/d} k_{th}^{thml,c/d}, \quad \forall t\in\mathcal{T}, h\in\mathcal{H} \tag{33}$$

where, $P_{th}^{thml,c/d}$ denotes the charging (c) or discharging (d) rate of thermal storage whereas $P_{\max,t}^{thml,c/d}$ is the maximum rate of the same. $k_{th}^{thml,c/d}$ is binary variable of the charging/discharging rate.

Also, simultaneous charge and discharge of the thermal storage is restricted by:

$$0 \le k_{th}^{thml,c} + k_{th}^{thml,d} \le 1, \quad \forall t\in\mathcal{T}, h\in\mathcal{H} \tag{34}$$

The following equation ensures an equal amount of usable heat between the first and last hour of operation planning:

$$E_0^{thml} = E_{24}^{thml} \tag{35}$$

where, E_0^{thml} and E_{24}^{thml} denotes the stored energy at the first and last hour, respectively.

6) Net energy balance: The next equation requires that the electricity generated match the yearly electric load at the facility across all electric loads, technologies, time stages, and fuel transporters (CHP and TES), necessitating the site to precisely attain electric net zero. During grid-isolated times, this load-balancing condition is specially imposed.

$$\sum_{d\in\mathcal{D}^E,t\in T,h\in\mathcal{H}} F_{dtlh}^p F_{ltd}^B X_{dtlhsu}^{rp} = \delta_l + \sum_{d\in\mathcal{D}^E,t\in\mathcal{T},h\in\mathcal{H}} P_{dtlhs}^E \tag{36}$$

where, F_{ltd}^B denotes the fixed fuel utilization. δ_l and P_{dtlhs}^E are indicators of annual and additional electric power consumption, respectively.

7) Network Constraints: The formulations presented in this section are predicated on the assumption that the proposed energy management scheme does not cause congestion or violate any network-related constraints, which is a common assumption in (EV) integrated microgrid research [2], [15], [17], [19], [21], [26]. However, depending on the network parameters, this claim is not always true. In order to include network constraints in the proposed method, power balancing constraints in (36) should be replaced by the following network power flow equations. Power flow constraints for integrated charging station:

$$-P_{ev}^{max} \le \sum_n e_n^t + P_{tlh} = X_t^g \le P_{ev}^{max} \tag{37}$$

where P_{ev}^{max} denotes the power flow limit for the EV charging station. e_n^t is the amount of charging/discharging power of n$^{\text{th}}$ EV ($e_n^t = e_n^{t+} - e_n^{t-}$).

Voltage constraint:

$$V_b^{min} \le V_b^t \le V_b^{max} \tag{38}$$

Bus constraints:

$$\begin{cases} -P_{G_b}^{max} \le P_{G_b}^t \le P_{G_b}^{max} \\ -Q_{G_b}^{max} \le Q_{G_b}^t \le Q_{G_b}^{max} \\ \quad \begin{cases} P_{xb}^t = -P_{bx}^t \\ Q_{xb}^t = -Q_{bx}^t \end{cases} \\ \begin{cases} -P_{bx}^- \le P_{bx}^t \le P_{bx}^{max} \\ -Q_{bx}^- \le Q_{bx}^t \le Q_{bx}^{max} \end{cases} \end{cases} \tag{39}$$

where b represents the bus where the integrated charging station is connected and if a whole power network is evaluated, x refers to all nearby buses. P_{Gb}^t and Q_{Gb}^t are the active and reactive power transaction from (+) or to (-) the grid connecting to the same bus b ($P_G^t = P_G^{t+} - P_G^{t-}$)

C. Resilience evaluation

Energy Resilience is a complicated and vast process in and of itself, and this study does not consider 'infrastructure' resilience, instead focuses on improving 'operational' resilience. While we recognize the importance of the planning and adaptation stages, our primary focus in this work is on absorption and, to a lesser extent, the recovery capability of the mMG. To evaluate the resilience of the system, operationally stochastic and energy-based metrics are developed for the restoration of critical loads as well as power system infrastructure (e.g., damaged poles and lines) [35]. The system resilience is defined in the time period [h_s, h_e] as:

$$R = \int_{h_s}^{h_e} \sum_{c\in C} W_c P_c(h) \mathrm{d}h \tag{40}$$

where C is the set of critical loads restored by microgrids, W_c is the weight of a critical load c, and $P_c(h)$ is the active power of load c at time h. In particular, the resilience of the system is measured in terms of probability of outage survival which is given as following:

$$\widehat{Prob}(h) = \prod_{i:h_i\le h} \left(1 - \frac{d_i}{n_i}\right) \tag{41}$$

where h_i the time when at least one outage occurred, d_i is the number of outage at time h_i, and n_i different combinations of mMGs that survived up to time h_i.

D. Integrated framework

The integrated overall optimization problem can be represented as follows:

$$\min C_{tot} \tag{42}$$

subject to (2)-(6), (13), (20)-(39).

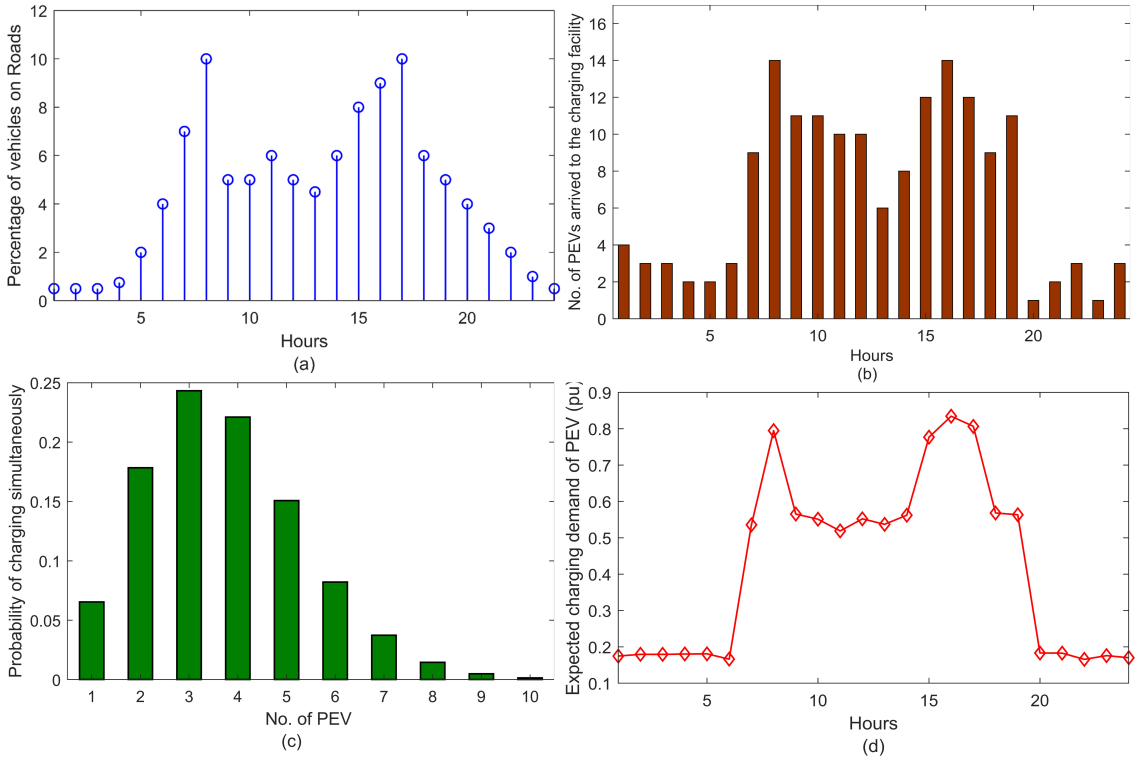

Fig. 4. Hourly simulation result of different status of EVs on a single day: (a) percentage of vehicles on roads per hour, (b) number of vehicles arrived to the charging station, (c) simultaneous charging probability of Evs, and (d) expected energy demand of the vehicles.

V. Case Studies

A. Test System and assumptions

We present a methodology for assessing a multi-energy microgrid's optimal size and operation strategy. Programmed on Python-based Pyomo language [36] in a desktop computer with Intel core-i7 3.20 GHz processor and 8 GB RAM, the Gurobi optimizer is used to solve the MILP optimization model.

Okinawa, a prefecture in Japan, is prone to natural disasters. Every year, several typhoons hit this island, among other calamities. The formulated approach is tested in hospitals in Nishihara, a city in Okinawa. We expect the model to have smooth islanding capacity in the event of an emergency, such as blackouts, because it is a grid-connected microgrid. The hospital's heating and electrical load demands are respectively 12,242 MMBtu and 7.75 MW. Fig. 5 shows the load profiles. The hospital's average electrical demand is 885.02 kW, with a minimum of 555.08 kW (April 06) and a maximum of 1427.33 kW (September 28). With an average load of 1.40 MMBtu/hr, the hospital has the highest demand on January 2 (4.63 MMBtu/hr) and the least demand on September 28 (0.06 MMBtu/hr). Okinawa Electric Power Company is considered the power supply provider. In this study, the net energy metering was not taken into account, such that after charging and satisfying demands, the extra energy produced by the PV unit would be curtailed. Furthermore, the fuel (natural gas) supply is expected to be uninterruptible throughout the operation of the CHP and boiler unit. This study did not consider net energy metering in order to keep the model simple and feasible.

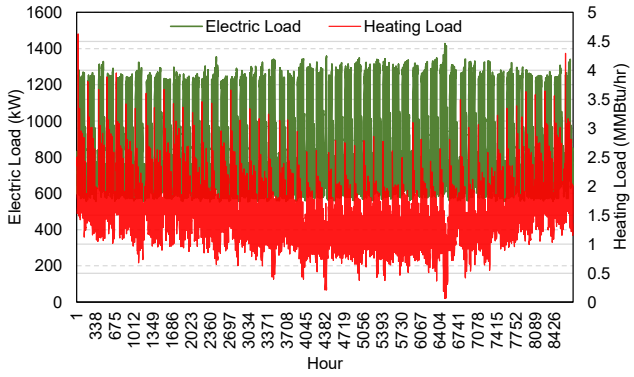

Fig. 5. Hourly Electrical and heating load profile of the test system

We employ electrical load profiles based on reports from the US DOE Commercial Reference Buildings (new construction) to capture the weekly and seasonal effects in the analysis, and hot water usage is encapsulated for the thermal load profile. The energy storage technology and associated cost characterization information is taken from [37]. The model optimizes the battery power (kW-AC) and capacity (kWh) separately for economic performance and resiliency. To calculate the output of PV generation, we use PVWatts, a program developed by NREL.

We assume that the EVs that are connected to the microgrid are electric ambulances (EA). This model assumes the usage of level-3 DC fast chargers with a maximum charging current

TABLE II
TEST CASES

Scenario	Case	EV	Resilience	Technologies
S1	1	No	No	ES+PV
	2	Yes	No	ES+PV
	3	No	Yes	ES+PV
	4	Yes	Yes	ES+PV
S2	5	No	No	ES+PV+CHP+TES
	6	Yes	No	ES+PV+CHP+TES
	7	No	Yes	ES+PV+CHP+TES
	8	Yes	Yes	ES+PV+CHP+TES
S3	9	No	No	CHP+TES
	10	Yes	No	CHP+TES
	11	No	Yes	CHP+TES
	12	Yes	Yes	CHP+TES

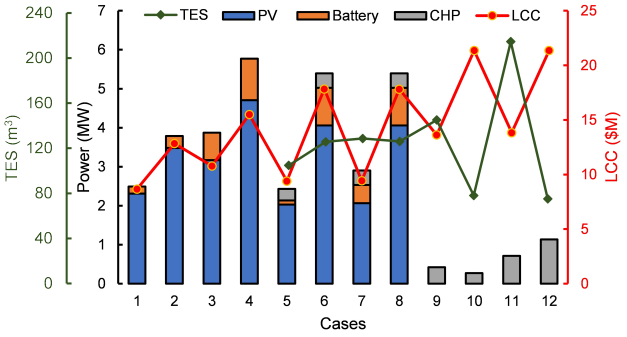

Fig. 6. Optimal size and life cycle cost for different cases

of 63 A and a charging voltage of 400 V. To determine the total predicted charging power of EVs, we first compute the charging current of each EV. The charging power of a single EV is then calculated. Fig. 4 shows the hourly values of vehicles on the road (%), the number of vehicles arriving at the charging station, and finally, the total expected EV charging demand is measured and integrated into the hospital microgrid.

In this analysis, the critical load is set at 50% of the total load. The outage is estimated to last 24 hours at this time. The assigned outage case is expected to be a major outage that occurs once every 25 years during the life of mMG.

B. Results

The test cases are divided into three scenarios in terms of technology selection. Each scenario has two parameters- with or without considering EV and resiliency that makes total 12 test cases as seen in Table II.

Fig. 6 refers to the optimal sizing results and system costs of different cases. The average optimal size of PV for S1 is around 11.9% greater than for S2. Also, average battery size of PV for S2 is less than S1 by about 10.8%. The reason behind this is quite obvious- the microgrid load demand of S2 is met by CHP and TES along with PV and battery. In terms of CHP and TES sizing, S4 has nearly 81% and 5% more capacity than S3, respectively. This is because the CHP needs to supply the load demand solely with a little help from TES and gas boiler.

S1 has a lower average cost than S2 and S3 by about 14% and 46.9%, respectively, even with the grid outages and electric vehicles. The primary reason for this is the high cost

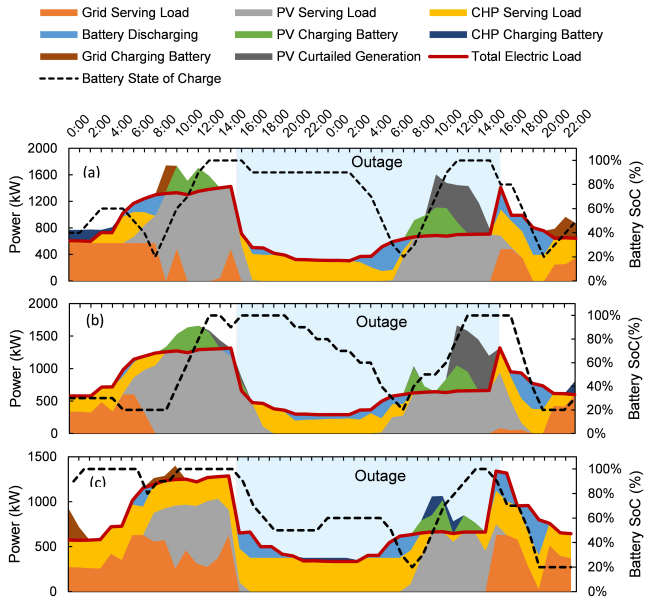

Fig. 7. Electrical Energy dispatch of case 7 under 24 hour outage during: (a) peak load demand in September, (b) summer solstice in July, (c) winter solstice in December

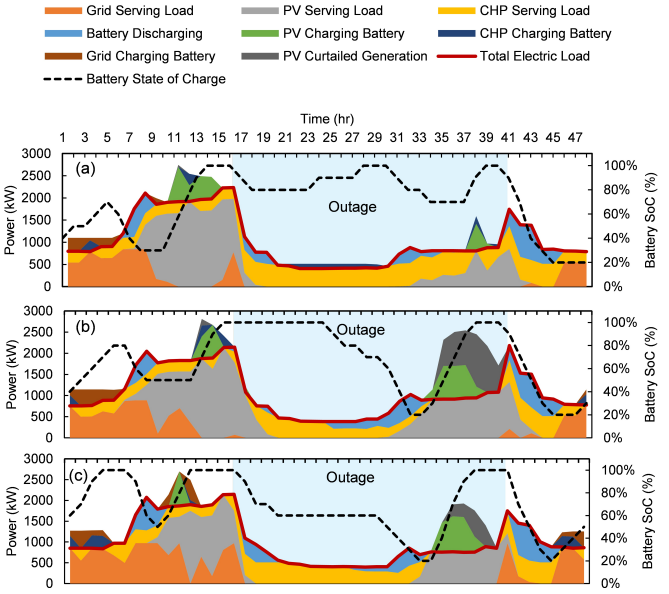

Fig. 8. Electrical Energy dispatch of case 8 under 24 hour outage during: (a) peak load demand in September, (b) summer solstice in July, (c) winter solstice in December

of the CHP unit. Regardless of resilience approach, the cost of integrating EV into the system is always higher than the case without EV. For example, the cost of case 6 that integrates EV is almost double than case 5 considering the normal operation of the grid. Again, case 8 is almost 89% more expensive compared to case 7 considering the power cut.

The following subsections describe the hourly dispatch strategy for electrical and heating energy balance under a pre-defined 24 hour outage in the months of July, September, and December. The outage periods are shaded in the corresponding

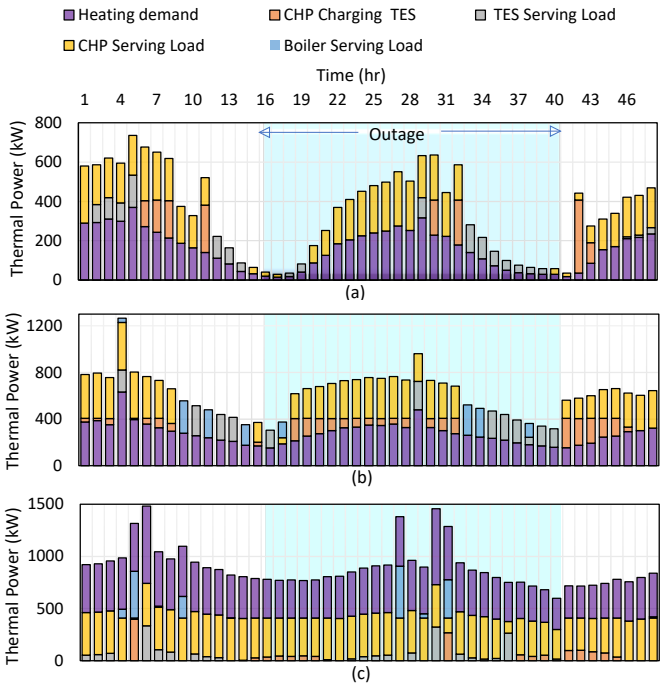

Fig. 9. Heat Energy dispatch of case 7 under 24 hour outage during: (a) peak load demand in September, (b) summer solstice in July, (c) winter solstice in December

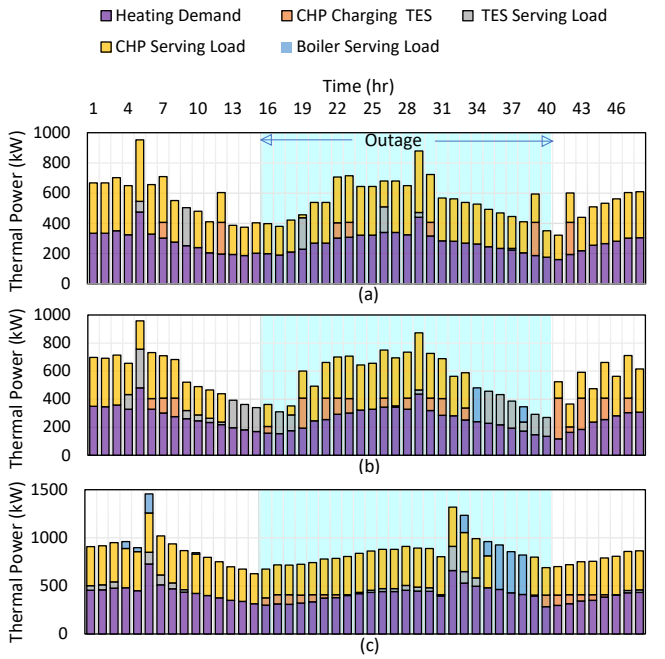

Fig. 10. Heat Energy dispatch of case 8 under 24 hour outage during: (a) peak load demand in September, (b) summer solstice in July, (c) winter solstice in December

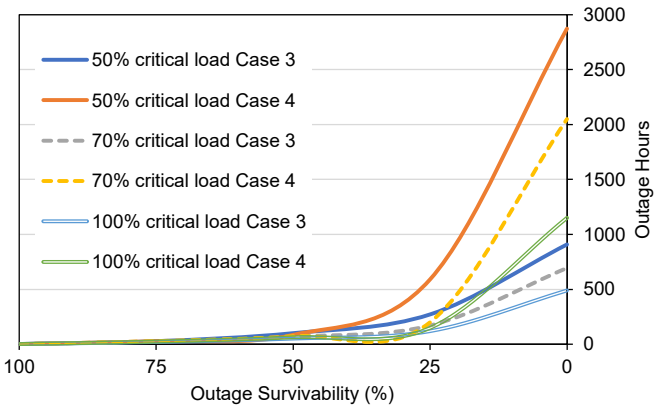

Fig. 11. Probability of outage survival for different critical load demand

figures.

1) Electrical energy dispatch: The dispatch strategy of each type of power generation for case 7 is shown in Fig. 7. During winter, most of the electricity demand is covered by CHP as heating demand is more than 1.5 times that of the summer season. Taking a two-day sample both in July and December, it is found that PV and the grid are the main energy suppliers, respectively, for case 7. This is the same for case 8 as shown in Fig. 8 irrespective of EV load. In fact, the grid contribution is 1.57 times higher in December than in July, whereas PV produces 1.66 times more in July compared to December. Although the CHP supply is almost the same for both cases, there is a significant difference in PV production. In fact, case 7 uses 16.5 percent and 12.2 percent less PV power to support the microgrid load. This is because of the exclusion of EVs and the economic dispatch strategy of the microgrid model. In all seasons and loading conditions, this phenomenon results in lower and higher PV curtailment for cases 7 and 8, respectively. The battery dispatch follows an almost identical trend for both cases, considering the outage and normal grid operation period. However, it should be noted that the outage starting time and percentage of critical load have a great impact on the dispatch strategy of the energy storage along with other factors.

2) Heating energy dispatch: Figure 9 and 10 show the hourly heating energy dispatch of case 7 and 6, respectively. CHP always takes the lead when it comes to heating energy delivery for all cases. Interestingly, TES serves the heat demand primarily in July, followed by December and September in both cases. This is because in the summer (July), CHP is preoccupied with serving both electric and heat loads at the same time. When both CHP and TES are unable to meet the load demand, the boiler steps in as a backup. The boiler also takes over if the CHP is not available due to maintenance and such. CHP is responsible for charging the hot water TES in addition to supplying heat. There is no impact of other power generators such as grid, PV and battery as they are not involved in serving heat demand.

C. Outage survivability

Our outage survivability model is exponential, rather than non- or semi-parametric. Six cases (3, 4, 7, 8, 11, and 12) out of 12 in three scenarios are considered resilient, meaning they have all survived a 24-hour blackout. However, the probability of outage survival is not the same for all cases. Fig. 11 shows the outage survivability (%) for case 2 and 3. Because the

system model suggests a larger optimal size for the battery and PV in case 4 due to the integration of EVs, it has a higher survival hours than case 3. It should be noted that the survival outage hours vary depending on the critical load demand, and the higher the critical demands, the lower the survival hours.

D. Recommended financing

According to the findings, case 7 is the best option in terms of the total cost and resilience approach. The winning system includes 2,066 kW of PV, a 468 kW battery, and 371 kW of CHP with 128.67m^3 of thermal energy storage. However, if EV integration is considered along with the least total cost and resilience approach, case 8 stands out. The system size of this case is 4,061 kW of PV, 963 kW of battery unit, 368 kW CHP with 126m^3 TES. It is worth noting that, while case 1 has the lowest cost of all the test cases, it excludes the heating load demand.

VI. Conclusion and future work

In this work, an optimal multi-energy microgrid is proposed that satisfies both the electrical and heating load demand. Formulated as a mixed integer linear program (MILP), it reduces the total cost while measuring the outage survivability for prolonged grid blackouts. A smart EV charging station is modeled as well and integrated with the microgrid. The performance of the proposed method is examined using real load data from a hospital in Japan. It captures the efficiency benefits from waste heat recovery via the CHP unit by modeling the interaction of electrical and heat sources and imposing several practical constraints. A total of twelve cases are evaluated, divided into three scenarios in terms of EV integration and resiliency approach. The results showed the robust dispatch of the microgrid as it sustained the prolonged grid blackout regardless of technology selection, seasonal variability (winter, summer and peak) and EV integration. Case 8 with battery, PV, CHP and thermal storage appeared to be the best option, satisfying all of the assessing criteria such as heating and electrical load demand, EV charging need, and endurance against extreme events, with an acceptable size and life cycle cost of the participating technology mix. In the future, the proposed methodology could be extended to other vulnerable critical facilities such as schools, data centers, airports, water treatment plants, and so on. Net energy metering, demand response, and cooling load can be added to the proposed microgrid model as well. To investigate system resilience, probabilistic techniques can be used with historical blackout and brownout data as well.

References

[1] A. T. D. Perera, V. M. Nik, D. Chen, J. Scartezzini, and T. Hong. Quantifying the impacts of climate change and extreme climate events on energy systems . *Nat. Energy*, 5(2):150–159, Feb 2020.

[2] H. Mehrjerdi, R. Hematti, S. Mahdavi, M. Shafie-khah, and J. P. S. Catalao. Multi-Carrier Microgrid Operation Model using Stochastic Mixed Integer Linear Programming. *IEEE Trans. Ind. Inf.*, Oct 2021.

[3] Y. Wang, J. Chen, C.and Wang, and R. Baldick. Research on resilience of power systems under natural disasters—a review. *IEEE Trans. Power Systems*, 31(2):1604–1613, 2016.

[4] A. Gholami, T. Shekari, and S. Grijalva. Proactive management of microgrids for resiliency enhancement: An adaptive robust approach. *IEEE Trans. Sustain. Energy*, 10(1):470–480, 2019.

[5] B. Chen, X. Wang, J.and Lu, C. Chen, and S. Zhao. Networked microgrids for grid resilience, robustness, and efficiency: A review. *IEEE Trans. on Smart Grid*, 12(1):18–32, 2021.

[6] A. Umunnakwe, H. Huang, K. Oikonomou, and K. R. Davis. Quantitative analysis of power systems resilience: Standardization, categorizations, and challenges. *Renewable Sustainable Energy Rev.*, 149:111252, Oct 2021.

[7] A. Hussain, V. Bui, and H. Kim. Resilience-oriented optimal operation of networked hybrid microgrids. *IEEE Trans. Smart Grid*, 10(1):204–215, 2019.

[8] A. Khodaei. Resiliency-oriented microgrid optimal scheduling. *IEEE Trans. Smart Grid*, 5(4):1584–1591, 2014.

[9] S. D. Manshadi and M. E. Khodayar. Resilient operation of multiple energy carrier microgrids. *IEEE Trans. Smart Grid*, 6(5):2283–2292, 2015.

[10] H. Xie, X. Teng, Y. Xu, and Y. Wang. Optimal energy storage sizing for networked microgrids considering reliability and resilience. *IEEE Access*, 7:86336–86348, 2019.

[11] H. Masrur, A. Sharifi, M. R. Islam, M. A. Hossain, and T. Senjyu. Optimal and economic operation of microgrids to leverage resilience benefits during grid outages. *Intl. Journal of Elec. Power & Energy Syst.*, 132:107137, 2021.

[12] JAMA - Japan Automobile Manufacturers Association, Inc [online] Available: http://www.jama-english.jp.

[13] Charging Equipment Introduction Promotion Project [online]. Available: https://www.tokyo-co2down.jp/subsidy/mansion-evcharge.

[14] Abir Muhtadi, Dilip Pandit, Nga Nguyen, and Joydeep Mitra. Distributed Energy Resources Based Microgrid: Review of Architecture, Control, and Reliability. *IEEE Trans. Ind. Appl.*, 57(3):2223–2235, Mar 2021.

[15] J. Cao, C. Crozier, M. McCulloch, and Z. Fan. Optimal design and operation of a low carbon community based multi-energy systems considering ev integration. *IEEE Trans. Sustain. Energy*, 10(3):1217–1226, 2019.

[16] M. S. Rahman, M. J. Hossain, J. Lu, F. H. M. Rafi, and S. Mishra. A Vehicle-to-Microgrid Framework With Optimization-Incorporated Distributed EV Coordination for a Commercial Neighborhood. *IEEE Trans. Indl. Informat.*, 16(3):1788–1798, 2020.

[17] H. Farzin, M. Fotuhi-Firuzabad, and M. Moeini-Aghtaie. Reliability Studies of Modern Distribution Systems Integrated With Renewable Generation and Parking Lots. *IEEE Trans. Sustain. Energy*, 8(1):431–440, Aug 2016.

[18] M. F. Shaaban, S. Mohamed, M. Ismail, K. A. Qaraqe, and E. Serpedin. Joint planning of smart ev charging stations and dgs in eco-friendly remote hybrid microgrids. *IEEE Trans. Smart Grid*, 10(5):5819–5830, 2019.

[19] J. Van Roy, N. Leemput, F. Geth, J. Büscher, R. Salenbien, and J. Driesen. Electric vehicle charging in an office building microgrid with distributed energy resources. *IEEE Trans. Sustain. Energy*, 5(4):1389–1396, 2014.

[20] Qin Yan, Bei Zhang, and Mladen Kezunovic. Optimized Operational Cost Reduction for an EV Charging Station Integrated With Battery Energy Storage and PV Generation. *IEEE Trans. Smart Grid*, 10(2):2096–2106, Jan 2018.

[21] Mahmoud M. Gamil, Tomonobu Senjyu, Hasan Masrur, Hiroshi Takahashi, and Mohammed Elsayed Lotfy. Controlled V2Gs and battery integration into residential microgrids: Economic and environmental impacts. *Energy Convers. Manage.*, 253:115171, Feb 2022.

[22] Vivek Mohan, Jai Govind Singh, and Weerakorn Ongsakul. Sortino Ratio Based Portfolio Optimization Considering EVs and Renewable Energy in Microgrid Power Market. *IEEE Trans. Sustainable Energy*, 8(1):219–229, Jul 2016.

[23] Furkan Ahmad, Mohammad Saad Alam, Samir M. Shariff, and Mahesh Krishnamurthy. A Cost-Efficient Approach to EV Charging Station Integrated Community Microgrid: A Case Study of Indian Power Market. *IEEE Trans. Transp. Electrif.*, 5(1):200–214, Jan 2019.

[24] Akhtar Hussain, Van-Hai Bui, and Hak-Man Kim. Optimal Sizing of Battery Energy Storage System in a Fast EV Charging Station Considering Power Outages. *IEEE Trans. Transp. Electrif.*, 6(2):453–463, Mar 2020.

[25] Zhirong Shen, Changle Wu, Lin Wang, and Guanglin Zhang. Real-Time Energy Management for Microgrid With EV Station and CHP Generation. *IEEE Trans. Network Sci. Eng.*, 8(2):1492–1501, Mar 2021.

[26] Mingrui Zhang and Jie Chen. The Energy Management and Optimized Operation of Electric Vehicles Based on Microgrid. *IEEE Trans. Power Delivery*, 29(3):1427–1435, May 2014.
[27] Adhithya Ravichandran, Shahin Sirouspour, Pawel Malysz, and Ali Emadi. A Chance-Constraints-Based Control Strategy for Microgrids With Energy Storage and Integrated Electric Vehicles. *IEEE Trans. Smart Grid*, 9(1):346–359, Apr 2016.
[28] B. Yan, P. B. Luh, G. Warner, and P. Zhang. Operation and design optimization of microgrids with renewables. *IEEE Trans. Autom. Sci. Eng.*, 14(2):573–585, 2017.
[29] H. Masrur, M. M. Gamil, M. R. Islam, K. M. Muttaqi, M. S. H. Lipu, and T. Senjyu. An Optimized and Outage-resilient Energy Management Framework for Multi-carrier Energy Microgrids Integrating Demand Response. *IEEE Trans. Ind. Appl.*, 58(3):1–10, Mar 2022.
[30] H. Masrur, T. Senjyu, M. R. Islam, A. Z. Kouzani, and M A P. Mahmud. Resilience-oriented dispatch of microgrids considering grid interruptions. *IEEE Trans. Appl. Supercond.*, 31(8):1–5, 2021.
[31] W. Violante, C. A. Cañizares, M. A. Trovato, and G. Forte. An energy management system for isolated microgrids with thermal energy resources. *IEEE Trans. Smart Grid*, 11(4):2880–2891, 2020.
[32] R. Bahmani, H. Karimi, and S. Jadid. Cooperative energy management of multi-energy hub systems considering demand response programs and ice storage. *Int. J. Electr. Power Energy Syst.*, 130:106904, Sep 2021.
[33] O. Hafez and K. Bhattacharya. Queuing analysis based pev load modeling considering battery charging behavior and their impact on distribution system operation. *IEEE Trans. Smart Grid*, 9(1):261–273, 2018.
[34] M. Keskin, G. Laporte, and B. Çatay. Electric Vehicle Routing Problem with Time-Dependent Waiting Times at Recharging Stations. *Computers & Operations Research*, 107:77–94, Jul 2019.
[35] H. Gao, Y. Chen, Y. Xu, and C. Liu. Resilience-oriented critical load restoration using microgrids in distribution systems. *IEEE Trans. Smart Grid*, 7(6):2837–2848, 2016.
[36] Michael L. Bynum, Gabriel A. Hackebeil, William E. Hart, Carl D. Laird, Bethany L. Nicholson, John D. Siirola, Jean-Paul Watson, and David L. Woodruff. *Pyomo–optimization modeling in python*, volume 67. Springer Science & Business Media, third edition, 2021.
[37] Energy Storage Technology and Cost Characterization Report | PNNL [online]. Available: https://www.pnnl.gov/publications/energy-storage-technology-and-cost-characterization-report.

Hasan Masrur earned a Master's Degree in Electric Power System Management from the Department of Energy, Environment, and Climate Change at the Asian Institute of Technology (AIT) in Thailand in 2017. He is currently pursuing a Ph.D. in Interdisciplinary Intelligent Systems Engineering at the University of the Ryukyus, Okinawa, Japan. He has been involved in a number of research projects in both academia and industry. Throughout his academic career, he has received several research grants, including the Marubun Exchange Research Grant, and scholarships, including one from the Japanese government (Monbukagakusho: MEXT).His research interests are in the areas of optimization, resilience, and techno-economics of energy systems; energy management strategies; load and demand side management; microgrids and smart grids; renewable and sustainable energy technologies; energy storage systems; and power system dynamics, stability, and control. His research findings have been published in several peer-reviewed journals and conference proceedings.

Miadreza Shafie-khah (SM'17) received his first PhD in electrical engineering from Tarbiat Modares University, Tehran, Iran. He received his second PhD in electromechanical engineering and first postdoc from the University of Beira Interior (UBI), Covilha, Portugal. He received his second postdoc from the University of Salerno, Salerno, Italy. Currently, he is an Associate Professor at the University of Vaasa, Vaasa, Finland. He is an Editor of the IEEE TRANSACTIONS ON SUSTAINABLE ENERGY, an Associate Editor of the IEEE Systems Journal, an Associate Editor of the IEEE Access, an editor of the IEEE Open Access Journal of Power and Energy (OAJPE), an Associate Editor for IET-RPG, and the guest Editor-in-Chief of the IEEE OAJPE. He is a Top Scientist in the Research.com Ranking in Engineering and Technology, and he has won five Best Paper Awards at IEEE Conferences. His research interests include electricity markets, power system optimization, demand response, electric vehicles, price and renewable forecasting and smart grids.

M. Jahangir Hossain (M'10-SM'13) received the B.Sc. and M.Sc. Eng. degrees from Rajshahi University of Engineering and Technology (RUET), Bangladesh, in 2001 and 2005, respectively, and the Ph.D. degree from the University of New South Wales in 2010, Australia, all in electrical and electronic engineering. He is currently an Associate Professor with the School of Electrical and Data Engineering, University of Technology, Sydney, Australia. Before joining there, he served as an Associate Professor in the School of Engineering, Macquarie University, Senior Lecturer and a Lecturer in the Griffith School of Engineering, Griffith University, Australia for five years and as a Research Fellow in the School of Information Technology and Electrical Engineering, University of Queensland, Brisbane, Australia. His research interests include renewable energy integration and stabilization, voltage stability, micro grids and smart grids, robust control, electric vehicles, building energy management systems, and energy storage systems.

Tomonobu Senjyu (Senior Member, IEEE) was born in Saga, Japan, in 1963. He received the B.S. and M.S. degrees in electrical engineering from the University of the Ryukyus, Japan, in 1986 and 1988, respectively, and the Ph.D. degree in electrical engineering from Nagoya University, Nagoya, Japan, in 1994. He is currently a Full Professor in the Department of Electrical and Electronic Engineering at the University of the Ryukyus. He is currently serving as a member of the Science Council of Japan (SCJ). His research interests include renewable energy, power system optimization and operation, power electronics, and advanced control of electrical machines. His work attracted several research grants worth several million yen, and he published over 800 articles, including a number of IEEE Transactions.